Biophysical Journal, Volume *112*

Supplemental Information

Structural Behavior of the Peptaibol Harzianin HK VI in a DMPC Bilayer: Insights from MD Simulations

Marina Putzu, Sezgin Kara, Sergii Afonin, Stephan L. Grage, Andrea Bordessa, Grégory Chaume, Thierry Brigaud, Anne S. Ulrich, and Tomáš Kubař

I. METHODS

A. Force field, general simulation parameters, and starting structures

The needed sets of atomic charges for the non-standard residues Aib and Leuol were obtained by restrained electric potential fitting method (RESP)[1] with molecular electric potentials obtained on the HF/6-31G* level of theory, and the parameters for torsions along the backbone dihedral angles of Aib were obtained by fitting to data generated on the B3LYP/TZVP level. Quantum chemical calculations were performed with Gaussian 09,[2] and the parameter and topology files for Aib and Leuol are attached to this Supporting Information as a zip archive (`Amber_files.zip`). Long-range electrostatic interactions were treated with the particle–mesh Ewald scheme (PME),[3] using a real-space cutoff of 1.0 nm, Fourier spacing of 0.12 nm and a fourth-order interpolation to the Ewald mesh. Van der Waals interactions were cut off at 1.0 nm. Long-range dispersion correction to the pressure and potential energy were considered.[4]

The leap-frog integrator was applied with a time step of 2 fs, and all of the covalent bonds were constrained by means of the LINCS algorithm.[5] All production simulations were performed in the NPT ensemble, where the temperature was kept constant with the Nosé–Hoover thermostat,[6,7] with solvent, peptide and lipid coupled to separate heat baths with coupling constants of 0.5 ps. The pressure was maintained constant with a semi-isotropic scheme, so that the pressure in the membrane plane was controlled separately from the pressure in the membrane normal direction, and the Parrinello–Rahman barostat[8] was applied with a reference pressure of 1 bar, a coupling constant of 2 ps, and a compressibility of 4.5×10^{-5} bar^{-1}. The coordinates of atoms were saved every 2 ps.

To build the structure of the system, use was made of a DMPC bilayer containing 128 molecules (64 per leaflet) pre-equilibrated at 303 K, which was downloaded from the Slipids web site.[9] Two different protocols were employed to create the initial structures of the HZ–bilayer system: (i) The HZ molecule was placed in the aqueous phase and the pre-equilibrated DMPC bilayer was left intact. First, 5 ns of MD simulation were performed at 480 K, which led to the insertion of HZ into the bilayer within 2 ns. Then, the system was cooled down with further 40 ns of simulation with a reference temperature of 300 K. This procedure will be referred to as the heating–cooling protocol.[10] (ii) The structure of the HZ

molecule immersed in the DMPC bilayer was generated directly with Inflategro,[11] and an equilibration simulation of 40 ns was performed.

B. Free MD simulation

The initial structures of HZ were constructed with the xLeap program of the AmberTools package,[12] and the initial backbone dihedral angles applied are shown in Tab. I.

Conformation	Residue	φ	ψ	ω
α-helix		$-60°$	$-45°$	$180°$
3_{10}-helix		$-50°$	$-25°$	$180°$
β-bend	Xaa1	$-90°$	$-27°$	$180°$
	Yaa2	$-98°$	$-17°$	$180°$
	Aib3	$-49°$	$-50°$	$180°$
	Pro4	$-78°$	$+3°$	$180°$
extended		$180°$	$180°$	$180°$

TABLE I. Idealized backbone dihedral angles of the considered initial conformations of the HZ molecule. The values for the β-bend ribbon spiral taken from Ref. 13.

Some simulations involved additional restraints in order to keep the conformation of HZ close to the initial one. For the helical conformations, 3_{10} and α, these took the form of harmonic distance restraints on all of the backbone hydrogen bonds, $V(d) = \frac{1}{2}k(d - d_0)^2$ with d being the length of the hydrogen bond, and the parameters $k = 50$ kJ mol^{-1} Å^{-2} and $d_0 = 2.4$ Å. The two prolines in the HZ molecule cannot act as hydrogen donors, and in these cases, the restraints were applied to the distance b between the unsatisfied hydrogen acceptor (the amido oxygen atom of the amino acid three or four residues upstream, for 3_{10} and α, respectively) and the nitrogen of the proline, with $b = 4.0$ Å. For the β-bend ribbon structure, harmonic restraints of the form $V(\zeta) = \frac{1}{2}k(\zeta - \zeta_0)^2$ were applied on the backbone dihedral angles of the two motifs Xaa–Yaa–Aib–Pro, i.e., amino acid residues 3–10, with $k = 1.523$ kJ mol^{-1} deg^{-2}.

C. Experimental work

Peptide synthesis/purification. Two HZ peptides – a native sequence and the ^{15}N-labelled version ({^{15}N}HZ, Ac-Aib-Asn-Ile-Ile-Aib-Pro-{^{15}N}Leu-Leu-Aib-Pro-Leuol) for solid-state NMR – were synthesized using automated solid-phase peptide synthesis on a Liberty Blue CEM instrument. The synthesis was performed starting from H-L-leucinol-2-chlorotrityl resin. Fmoc strategy protocols were used and each amino acid was coupled two times. Diisopropylcarbodiimide/OxymaPur was employed as a coupling reagent. Coupling reactions for all amino acids were accomplished under conditions of microwave activation for 2 min at 90 °C except for the Fmoc-Aib-OH (at 50 °C for 10 min). Fmoc deprotections were carried out one time using 20% piperidine for 3 min at 75 °C, except for the Fmoc-Aib-OH (2× 10 min at 25 °C). N-terminal acetylation of the peptidyl resins was performed manually by a double treatment with acetic anhydride and N-methylmorpholine for 1 h at ambient temperature. The 1,2-aminoalcohol peptides were cleaved from the resin upon 4 treatments with the hexafluoro-2-propanol/dichloromethane (1:4, vol) mixture for 1 h. The crude peptides were purified (> 98% purity) by semi-preparative reverse phase (C18) high-performance liquid chromatography (HPLC) and characterized by reverse phase (C18) HPLC-mass spectrometry (ESI) and by analytical reverse phase (C18) HPLC, each time using gradient elution with water/acetonitrile mixtures supplemented with 0.1 % TFA as the ion-pairing agent.

Lipids. Saturated lipids – 1,2-dilauroyl-*sn*-glycero-3-phosphocholine (DLPC), 1,2-dimyristoyl-*sn*-glycero-3-phosphocholine (DMPC) and 1,2-dipalmitoyl-*sn*-glycero-3-phosphocholine (DPPC) – were obtained from Avanti Polar Lipids in the lyophilized powder form and used without further purification.

Solid-state NMR. {^{15}N}HZ was reconstituted into mechanically oriented DMPC bilayers at a peptide/lipid molar ratio (P/L) of 1/100. Ca. 30 mg of the MeOH co-solubilized peptide/lipid mixture were spread over 20 glass slides (7.5 mm × 18 mm × 0.06 mm) and the resulting films dried under vacuum. The slides were stacked and hydrated by incubation in 96% relative humidity at 48 °C overnight. The sample was wrapped in parafilm and a plastic foil to prevent drying.

Solid-state NMR (ssNMR) experiments were performed on an Avance III Bruker NMR spectrometer equipped with a 14.1 T widebore magnet. ^{31}P ssNMR spectra were acquired

at 242.9 MHz, using a Bruker flat-coil double-resonance ^{1}H/X probe, with a Hahn echo sequence (90° pulse of 5 μs; echo delay of 30 μs), employing ^{1}H SPINAL64 decoupling scheme during acquisition (decoupling strength 50 kHz). At least 256 scans were accumulated (acquisition time of 10 ms; recycle delay of 2 s). For ^{15}N-NMR, ^{1}H-^{15}N cross-polarization experiment using a CP-MOIST pulse sequence was performed at 60.8 MHz. The experiments were accomplished using a locally built double-tuned probe with a low-E flat-coil resonator, employing a ^{1}H and ^{15}N radiofrequency field strength of 65 kHz during the cross-polarization, and a 36 kHz ^{1}H SPINAL16 decoupling during acquisition. A mixing time of 250 μs was used, and 25600 scans were accumulated (acquisition time of 10 ms; recycle delay of 3 s). The ^{15}N chemical shift was referenced using the signal of a dry powder of ammonium sulfate, of which the chemical shift was set to 26.8 ppm. All NMR experiments were performed at 35 °C, i.e. above the DMPC phase transition temperature.

Synchrotron radiation circular dichroism (SRCD) spectroscopy. Measurements were carried out on the UVCD-12 beamline at the ANKA synchrotron facility at KIT.[14] For non-oriented CD, HZ was dissolved in 1:1 (vol.) mixture (50% TFE) of 2,2,2-trifluoroethanol and a salt-free 10 mM phosphate buffer (pH 7.4 at 25 °C) at the end concentration 8 mg·mL^{-1}. The sample was placed in a Hellma 12.5 μm thick circular CaF_2 cuvette. Three consecutive scans were collected and averaged at 30 °C. The scans were collected between 270 to 170 nm at a rate of 15 nm·min^{-1} with 0.5 nm intervals using 1.5 s dwell time and 1 nm bandwidth. After subtracting the baseline spectrum of the pure solvent, the averaged spectrum was converted to mean residue ellipticity. For oriented CD (SROCD), mixtures of HZ (ca. 8 μg) and respective lipid (strictly 200 μg) at P/L of 1/100 were prepared first as MeOH/$CHCl_3$ solutions. The solutions were allowed to dry on quartz glass plates, placed into a locally built SROCD sample cell and hydrated by incubation in 97% relative humidity overnight. One scan running at 15 nm·min^{-1} with 0.5 nm intervals using 1.5 s dwell time and 1 nm bandwidth for each of the eight 45° rotation positions from 0° to 315° was collected. The data were acquired from 270 to 175 nm at 30 °C under constant 97% relative humidity.

D. Additional HREX simulation

An additional HREX simulation was performed, starting from a different initial structure where the HZ molecule was placed in the aqueous phase. The HREX simulation ran for 1 μs, and involved 8 replicas with the scaling factors were in the interval $1 \ldots 0.5$, corresponding to effective temperatures from 300 K to 600 K. The cut-off distance for Lennard-Jones interactions was increased to 1.4 nm in this simulation.

E. Additional – Metadynamics Simulation

Metadynamics simulations,[15] optionally in its well-tempered variant,[16] were performed with Plumed 2.1.2 interfaced to Gromacs 5.0. The molecular mechanics parameters were the same as used for the free MD and HREX simulations, as were the initial positions and orientations (HZ placed outside the DMPC bilayer, with its axis parallel to the bilayer surface). The collective variables z and τ were considered, much the same as in the HREX simulations.

In the normal metadynamics simulations, Gaussian potentials of 1.5 kJ·mol^{-1} height were deposited every 1 ps or every 2 ps. The well-tempered metadynamics used two different values of the bias factor, 6 and 10, and Gaussians were deposited every 2 ps with an initial height of 1.2 kJ·mol^{-1}. For all of the simulations, the Gaussian width was set to 0.35 rad for τ and to 0.35 nm for z.

In all of the attempts, one of four different initial conformations of the peptide were employed: α-helix, 3_{10}-helix, fully extended and central-α. The first three structure were built according to the Methods section of the main text. The "central-α" conformation was constructed by modelling only the central part of the peptide in an α-helical conformation; that involved only two hydrogen bonds, Ile3–Leu7 and Ile4–Leu8. The considered hydrogen bonds were restrained during the entire simulations. This unusual conformation was motivated by preliminary NMR results.

F. Additional – Umbrella Sampling Simulation

One-dimensional umbrella sampling (US) simulations were employed to estimate the free energy, or potentials of mean force (PMF) along the distance in the z-direction of the center of mass (COM) of the HZ molecule from COM of the bilayer. This variable describes the transfer of the HZ molecule from the DMPC bilayer to the aqueous phase, and also from one bilayer/solvent interface to the center of the bilayer.

The range of the z-coordinate from 0 (corresponding to the center of the bilayer) to 30 Å (which is already far in the aqueous phase) was divided into 61 windows spaced by 0.5 Å. Two series of US simulations were performed, with different starting coordinates in all of the windows. In the first set, the starting structures were created by pulling COM of HZ placed initially in the center of the bilayer (I-state) along the z-direction. In the second set, the initial pulling simulation was started with the HZ molecule placed at the edge of the hydrophobic tail region parallel to the surface (S-state). The initial structures of the I- and S-states were taken from the output of the previously performed free MD simulations. Harmonic biasing potential with a force constant of 10 kJ mol^{-1} Å^{-2} was applied, and the simulation in each of the windows ran for 500 ns. The Gromacs `g_wham` tool was used to analyze the trajectories and construct the PMF.

II. RESULTS

A. Free simulation

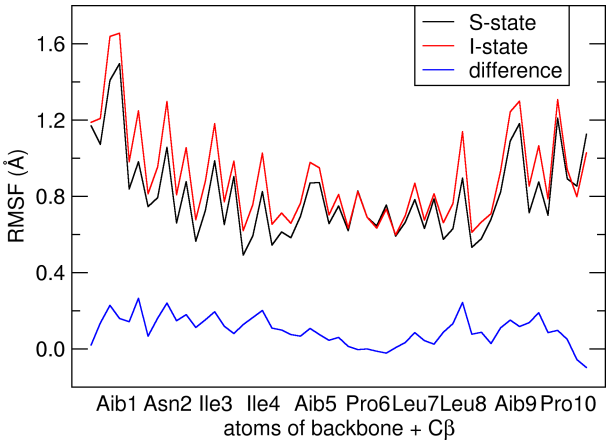

FIG. 1. Root mean square fluctuation (RMSF) of the individual atoms of backbones and Cβ of the HZ molecule in the S- and I-states, obtained from free MD simulations.

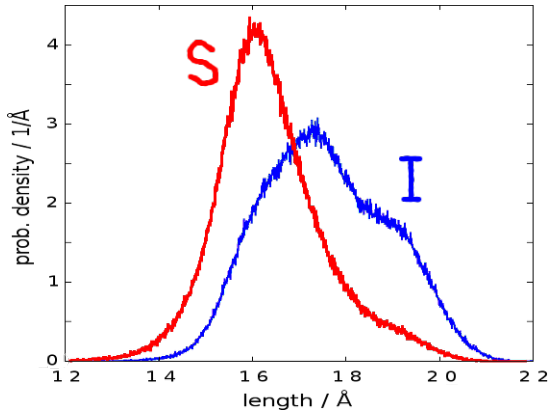

FIG. 2. Distribution of end-to-end length of the HZ molecule measured as the distance of the C_α of the first AA (Aib1) and the C_α of the last AA (Leuol11) in the MD trajectories of the S and I orientations.

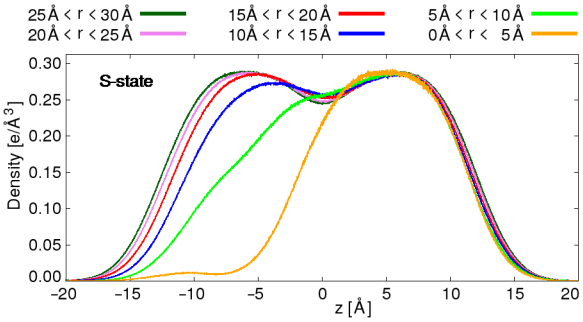

FIG. 3. Density profiles of the non-polar hydrocarbon tails of DMPC in the simulation of HZ in the S-state. The different profiles were obtained considering lipid atoms in the given ranges of horizontal distances from the center-of-mass of the HZ molecule. (Horizontal distance is the distance projected in the plane of bilayer surface.)

	S-state		I-state	
	φ	ψ	φ	ψ
Aib1	$-46°$	$-16°$	$-62°$	$-17°$
Asn2	$-65°$	$-22°$	$-71°$	$-25°$
Ile3	$-69°$	$-30°$	$-68°$	$-26°$
Ile4	$-86°$	$-31°$	$-83°$	$-15°$
Aib5	$-57°$	$-26°$	$-57°$	$-23°$
Pro6	$-61°$	$-23°$	$-61°$	$-15°$
Leu7	$-71°$	$-26°$	$-62°$	$-16°$
Leu8	$-99°$	$-17°$	$-76°$	$-14°$
Aib9	$-59°$	$-21°$	$-59°$	$-22°$
Pro10	$-66°$	$-20°$	$-68°$	$-14°$

TABLE II. Backbone dihedral angles of the dominant conformations of HZ observed in the unrestrained simulations of HZ immersed in the DMPC bilayer. Structures within 0.15 of each of the first two principal components were selected from the projection of each trajectory on the components obtained from principal component analysis performed on the combined trajectories. Presented are the averaged values of (φ, ψ) in these structural ensembles.

Root-mean-squared displacements of atomic positions (RMSD) of HZ with respect to static, idealized conformations were calculated along the MD trajectories. The idealized structures were $(\varphi, \psi) = (-74°, -4°)$ for 3_{10}, $(\varphi, \psi) = (-57°, -47°)$ for α, and considering the values of angles from Ref. 13 for β-bend ribbon. Only the fragment of the HZ molecule that may form a β-bend ribbon, consisting of the AAs Ile3–Pro10, was considered for this analysis, which was further restricted to the heavy atoms of the backbone.

reference	S-state	I-state
3_{10}-helix	1.25 ± 0.27	0.93 ± 0.30
β-bend ribbon	1.07 ± 0.24	1.10 ± 0.26
α-helix	1.40 ± 0.24	1.51 ± 0.28
average structure[a]	0.52 ± 0.20	0.58 ± 0.20

TABLE III. Root-mean-squared deviation (RMSD, in Å) of atomic positions of the HZ molecule with respect to selected reference structures, obtained from the MD trajectories with HZ molecule in the S and I orientations. The calculation of RMSD involved non-hydrogen atoms of the backbones of AAs 3 through 10. [a] Average structure taken from each respective MD trajectory.

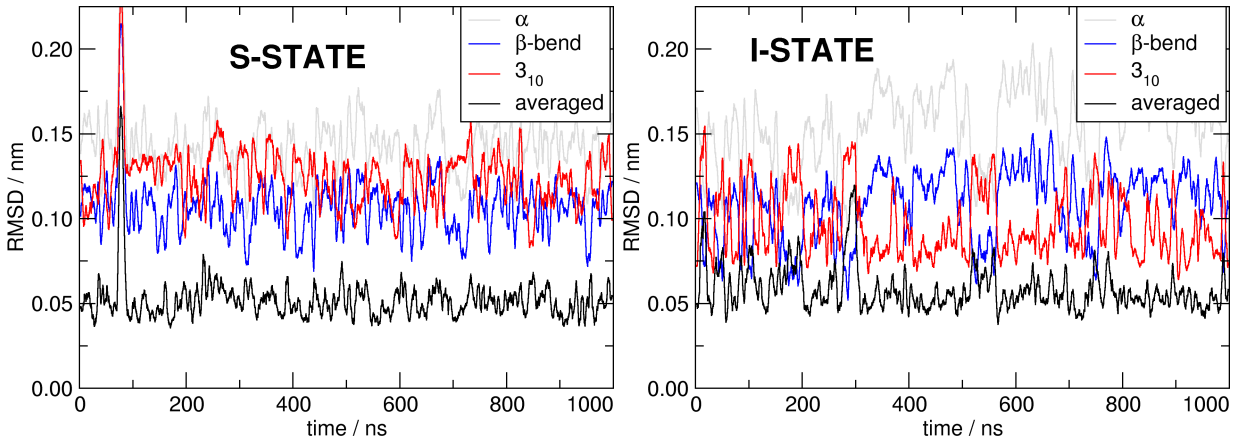

FIG. 4. Time course of RMSD of the HZ molecule with respect the selected reference structures, in the unrestrained simulations of the S-state (left) and the I-state (right). The calculation involved the heavy atoms of the backbones of amino acids 3 through 10.

B. Free simulation – convergence of HZ structure

A principal component analysis (PCA) was performed on the structural ensemble of the HZ molecule that was obtained by combination of the MD trajectories generated previously for HZ in the S- and I-states (1 μs each). Then, each of the two trajectories was projected into a two-dimensional space spanned by the first (PC1) and second eigenvectors (PC2) obtained from the PCA, see Fig. 5 for the projections. Note that the combination of PC1 and PC2 covers 72 % of structural variation of HZ in the structural ensemble combined from the simulations of S- and I-states. Also, we introduce a transformation of PC1 and PC2 into polar coordinates, as depicted in Fig. 5 also.

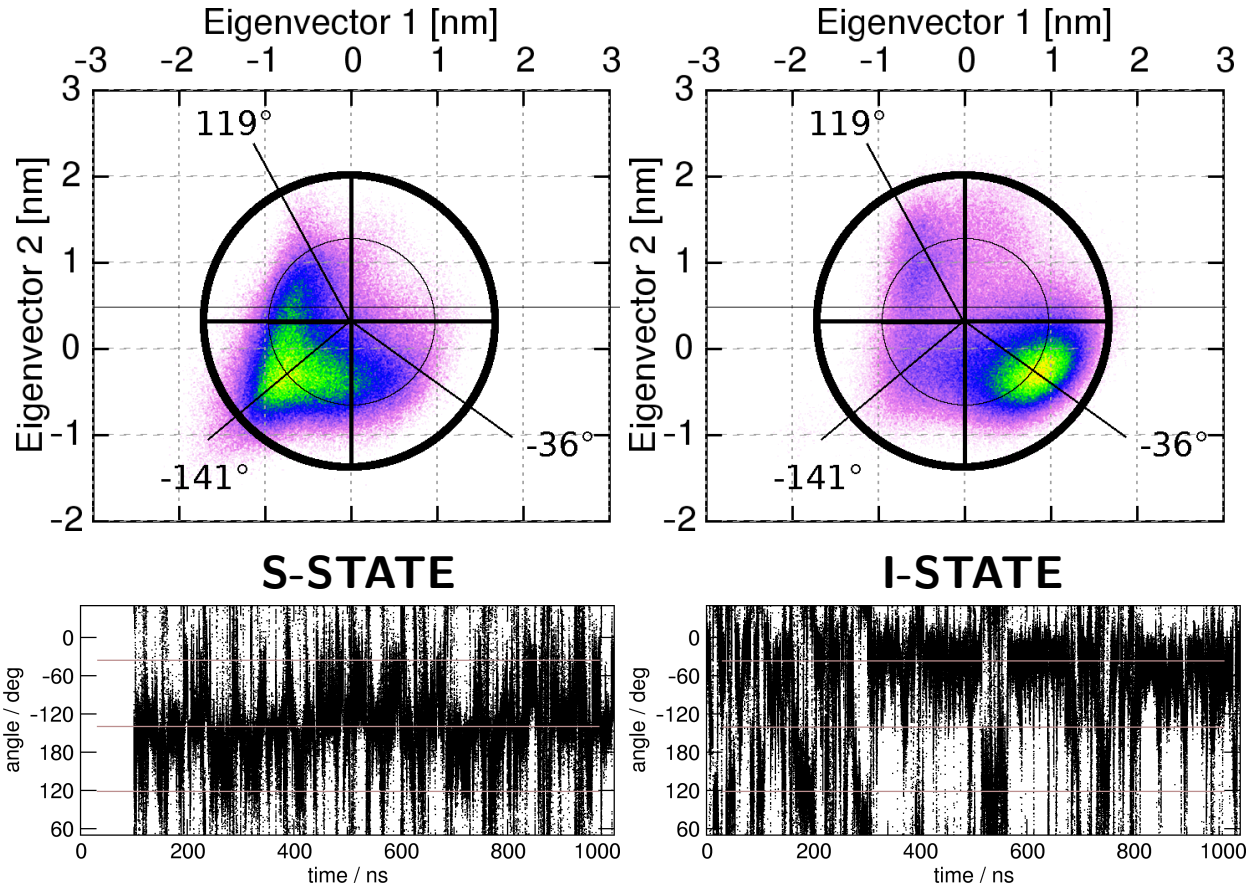

FIG. 5. Results from the principal component analysis. Top: Projection of each trajectory onto the first two eigenvectors, which were obtained from a PCA on the combined trajectories for the S- and I-states; Definition of the angular coordinate composed of PC1 and PC2, which makes it possible to distinguish between three structural states. Bottom: Time course of the angular coordinate in each of the trajectories.

The PCA plots reveal three different structural domains. Then, the structure at $-141°$ is dominant in the S-state, and the structure at $-36°$ dominates in the I-state, while the third structure at $119°$ is minor in both states. We use the angular coordinate obtained from PC1 and PC2 to assess the convergence of HZ structure in the free MD simulations performed.

On the assumption that three structural domains are possible, as identified above, it shall be checked whether interconvertions between them are observed during the simulation period. To this end, the angular coordinate is plotted along the respective MD trajectories in Fig. 5 (bottom). For the S-state, there are a number of transitions between $-141°$ and $-36°$, and $119°$ is populated transiently. The histogram of PC1/PC2 for the I-state features more clearly separated maxima, and the transitions between them are correspondingly more scarce; still, the dominantly populated $-36°$ is interrupted by interconversions to $-141°$ and $119°$ on multiple occasions. These observations confirm that the structural ensembles of HZ in the bilayer in both the S- and I-states are largely converged on the simulated time scale of 1 μs.

C. HREX simulation – convergence of orientation of HZ in the bilayer

Several interconversion between the S- and I-states are observed in the HREX simulation of 2 μs. This seems to be enough to provide a qualitatively correct free energy landscape (as presented in the main text), but even longer time scales would be required to obtain a statistically converged result.

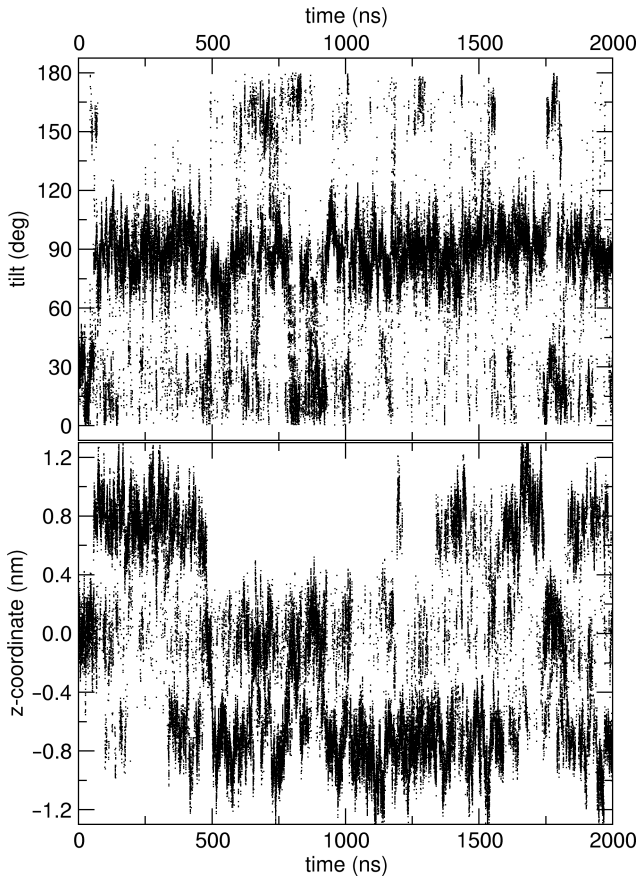

FIG. 6. The collective variables that describe the orientation of HZ in the DMPC bilayer, followed along the unperturbed replica ($\lambda = 1$) in the HREX simulation. The S-state is characterized by a tilt of 90° and z-coordinate of ca. +0.8 or −0.8 nm; the I-state exhibits a tilt close to 180° or −180° and z-coordinate of ca. 0.0 nm.

D. Additional HREX simulation

An additional HREX simulation was started with the HZ molecule located in the aqueous phase in all replicas, and the resulting free energy surface (FES) is shown in Fig. 7. Evidently, the deepest free energy minima are found in the aqueous phase, on both sides of the lipid bilayer. A minor minimum is found inside of the bilayer, corresponding to the S-state. In spite of the extended length of the simulations of 1 μs, convergence has not been reached apparently, for two reasons: Firstly, the free energy plot should be symmetric, meaning that if one of the S-states (with $z \approx 8$ Å) was found, the other one ($z \approx -8$ Å) would be expected as well. And, more importantly, the HZ molecule in the aqueous phase is predicted as the most likely state, which is entirely unexpected considering the purely non-polar character of HZ.

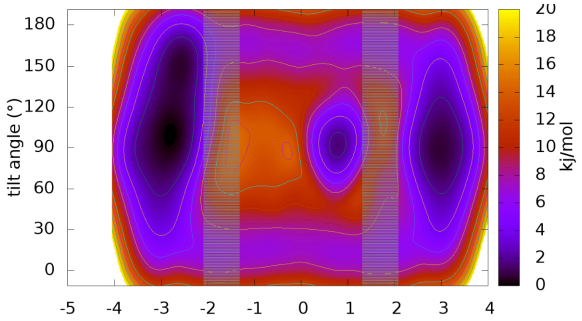

FIG. 7. Free energy surface from the HREX simulation with HZ molecule placed in the aqueous phase initially.

It seems that there is a rather high energy barrier opposing the insertion of HZ into the lipid bilayer, through the strongly polar lipid head group region. Then, the HZ molecule only passed into the hydrocarbon tail region late in the simulation, and the free energy minimum at $z \approx 8$ Å is only shallow. Also, the extremely rare interconversion between solvent and lipid bilayer, which only took place once in only one of the replicas, means that it is extremely difficult if not impossible to reach convergence of the free energy profile.

E. Additional – Free energies from metadynamics simulations

Relative free energies of the various orientations of the peptide molecule in the bilayer represent some of the most desirable quantities in a study like this. Unfortunately, this goal is difficult to achieve even with extended sampling techniques. This is best illustrated by our application of metadynamics simulation, with the intention to reach convergence of free energies in a two-dimensional representation. The orientation of the HZ molecule is described with the z-coordinate and the tilt angle, much the same as in the HREX simulations presented in the main text. In recent work by other authors, metadynamics simulations have been successful in the reconstruction of water/membrane partitioning free energy surfaces, in particular for small solutes.[17,18]

The same kind of calculation with a peptide, even a small one like HZ, in an atomistic lipid-water system is more challenging, and we are going to describe the problems that we were confronted with in these calculations. All of the attempted metadynamics simulations were either unstable or inefficient. Almost all of the normal metadynamics simulations crashed after ca. 100 ns. At this point, the underlying free energy surface was already filled with biasing Gaussians largely, and in fact, the motion along the collective variables (CV) became diffusive, see e.g. Fig. 8. A possible cause of the problem may lie in the singularities of the tilt angle at 0° and 180°; the diffusive dynamics along tilt may have led to an accelerated motion along the tilt CV and instabilities whenever the tilt became close to 0° or 180°. Unfortunately, even an analysis performed for the period of simulation preceding the crash never produced any reliable free energy surfaces.

The well-tempered metadynamics simulations behaved somewhat better, but still no convergence was reached. The bias deposition rate decreased over simulation time, and probably the bias factors used were too low, so that the system was unable to explore all of the FES. Changing the bias factor value from 6 to 10 did not bring any improvement, and it is difficult to choose the suitable bias factor because the relevant barrier heights are unknown. Still, the best results from the many attempts exhibited two minima associable to the S- and I-states, see Fig. 9.

There might be various reasons for such unsatisfactory results. The first concerns the representation of the two CVs. The tilt angle as defined here exhibits singularities at 0° and 180°. While this is no problem in a post-processing of a free or HREX simulation,

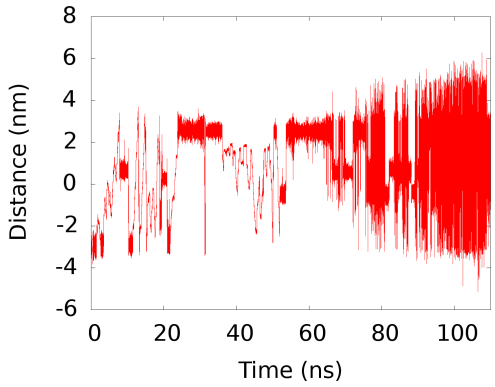

FIG. 8. Motion of the z CV during one of the normal metadynamics simulations of unrestrained HZ in a DMPC bilayer. The motion becomes diffusive after ca. 70 ns.

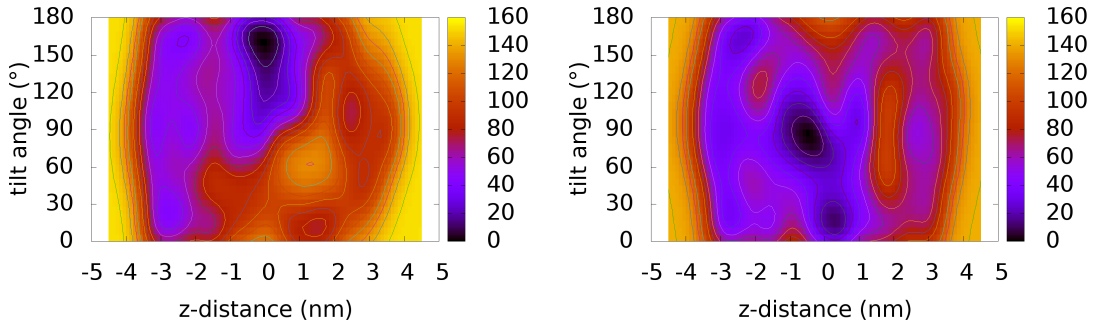

FIG. 9. Free energy surface from metadynamics well-tempered simulations with HZ molecule 3_{10}-helix restrained. The bias factor was set to 6 (left) and 10 (right).

it might become critical in a simulation with biasing potentials like metadynamics. A somewhat better choice might be the cosine of the tilt angle, and our further studies go in that direction. passing to the z-distance, this was defined relative to COM of all of the lipid. Such a definition may clearly lead to artifacts due to the undulations of the bilayer, which generate local deformations. Then, the COM of the entire bilayer does not describe the local neighborhood of the HZ molecule effectively. A better definition might be based on the lipid atoms within a cylinder aligned along the bilayer normal and centered on the solute.[19]

As mentioned above, even though the well-tempered simulations did not reach convergence, were be able to sample two minima of the FES, Surprisingly, only the peptide re-

strained to 3_{10}-helical conformation entered the hydrophobic region of the bilayer and really reached these minima. This means that the conformation of the peptide may be another important degree of freedom. Importantly, a dangerous caveat of metadynamics is that whenever such degrees of freedom, which are orthogonal to the biased CVs, are not sampled properly then the convergence becomes difficult, possibly leading to incorrect free energies.

In addition, another important phenomenon that is uncontrolled in the metadynamics simulation is the deformation or disruption of the bilayer that takes place as the peptide is being transferred from the aqueous phase to the interior of the bilayer. It seems to be very difficult to define a CV to control such structural changes, while it would be clearly orthogonal to the existing CVs, in the metadynamics language. A possible solution to that issue could be to combine metadynamics (with the present CVs) with HREX.

F. Additional – Free energies from umbrella sampling simulations

In another attempt to estimate free energies, we retorted to a one-dimensional representation and performed umbrella sampling simulations. The aim was to obtain the free energy profile for the HZ molecule approaching the center of the lipid bilayer and, on the other hand, being pulled out across the polar head-group layer into the aqueous solvent. The reaction coordinate was represented by the difference of the z-coordinate of COM of HZ and the z-coordinate of COM of the lipid bilayer. Two series of simulations were performed, each starting in on of the previously identified stable orientations of HZ, the S- and I-states. For each of the series, the reaction coordinate was divided into 60 windows spaced by 0.5 Å, and the starting structures for each of the windows were created from the respective stable state (S or I), by means of a rather fast non-equilibrium pulling simulation. Thus, the starting structures in each of windows were different in the S- and I-series of US simulations. It will turn out that this is an important point.

The free energy plots shown in Fig. 10 originate in series of US simulations of 500 ns per window, or 30 μs in total, for each of the I- and S-series, Apparently, even such an extensive sampling is insufficient to obtain a result that would be converged in the hydrocarbon tail region of $z = 0 - 1$ Å. The reason is that the orientation of the HZ molecule hardly changes during a simulation in a given window, and no interconversions between the S- and I-states are observed. Thus, each of the two series of US simulations provide its respective starting

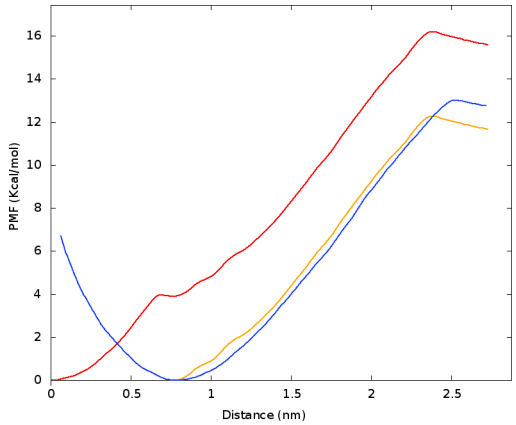

FIG. 10. Free energy profiles obtained from 1D umbrella sampling simulations of pulling HZ out of the bilayer into the aqueous phase. Starting structures generated by pulling simulations from two different structures; Red – starting from the I-state; orange – the same data, shifted vertically; blue – starting from the S-state.

structure as the more stable state – just because the respective other state is not sampled correctly.

On the other hand, both free energy profiles are very similar in the range of reaction coordinate above 10 Å. Seemingly, this provides a certain confidence to a rough estimate of the free energy cost of pulling the HZ molecule out of the membrane into the aqueous phase, which is around 11–13 kcal/mol on the basis of the US simulations performed. It would little surprise that such a largely non-polar molecule like HZ prefers the non-polar environment of the hydrocarbon tails to the polar solvent strictly. However, there might be a very similar problem as in the above reported metadynamics simulations – the deformation of the bilayer possibly leading to poor convergence, and thus to wrong free energies and hysteresis.

REFERENCES

[1]Bayly, C. I., P. Cieplak, W. D. Cornell, and P. A. Kollman, 1993. A well-behaved electrostatic potential based method using charge restraints for deriving atomic charges: The RESP model. *J. Phys. Chem.* 97:10269–10280.

[2]Frisch, M. J., G. W. Trucks, H. B. Schlegel, G. E. Scuseria, M. A. Robb, J. R. Cheeseman, G. Scalmani, V. Barone, B. Mennucci, G. A. Petersson, H. Nakatsuji, M. Caricato, X. Li, H. P. Hratchian, A. F. Izmaylov, J. Bloino, G. Zheng, J. L. Sonnenberg, M. Hada, M. Ehara, K. Toyota, R. Fukuda, J. Hasegawa, M. Ishida, T. Nakajima, Y. Honda, O. Kitao, H. Nakai, T. Vreven, J. A. Montgomery, Jr., J. E. Peralta, F. Ogliaro, M. Bearpark, J. J. Heyd, E. Brothers, K. N. Kudin, V. N. Staroverov, R. Kobayashi, J. Normand, K. Raghavachari, A. Rendell, J. C. Burant, S. S. Iyengar, J. Tomasi, M. Cossi, N. Rega, J. M. Millam, M. Klene, J. E. Knox, J. B. Cross, V. Bakken, C. Adamo, J. Jaramillo, R. Gomperts, R. E. Stratmann, O. Yazyev, A. J. Austin, R. Cammi, C. Pomelli, J. W. Ochterski, R. L. Martin, K. Morokuma, V. G. Zakrzewski, G. A. Voth, P. Salvador, J. J. Dannenberg, S. Dapprich, A. D. Daniels, O. Farkas, J. B. Foresman, J. V. Ortiz, J. Cioslowski, and D. J. Fox. Gaussian 09 Revision C.01. Gaussian Inc. Wallingford CT 2009.

[3]Darden, T., D. York, and L. Pedersen, 1993. Particle mesh Ewald – an $n \cdot \log(n)$ method for Ewald sums in large systems. *J. Chem. Phys.* 98:10089–10092.

[4]Gromacs reference manual, version 2016, section 4.9.1. http://manual.gromacs.org/documentation/2016/manual-2016.pdf, last accessed 7 Sep 2016.

[5]Hess, B., H. Bekker, H. J. C. Berendsen, and J. G. E. M. Fraaije, 1997. LINCS: A linear constraint solver for molecular simulations. *J. Comput. Chem.* 18:1463–1472.

[6]Nosé, S., 1984. A molecular dynamics method for simulations in the canonical ensemble. *Mol. Phys.* 52:255–268.

[7]Hoover, W. G., 1985. Canonical dynamics: Equilibrium phase-space distributions. *Phys. Rev. A* 31:1695–1697.

[8]Nosé, S., and M. L. Klein, 1983. Constant pressure molecular dynamics for molecular systems. *Mol. Phys.* 50:1055–1076.

[9]Jämbeck, J. P. M., and A. P. Lyubartsev, 2012. Derivation and Systematic Validation of a Refined All-Atom Force Field for Phosphatidylcholine Lipids. *J. Phys. Chem. B*

116:3164–3179.

[10]Ulmschneider, J. P., J. C. Smith, M. B. Ulmschneider, A. S. Ulrich, and E. Strandberg, 2012. Reorientation and dimerization of the membrane-bound antimicrobial peptide PGLa from microsecond all-atom MD simulations. *Biophys. J.* 103:472–482.

[11]Kandt, C., W. L. Ash, and D. P. Tieleman, 2007. Setting up and running molecular dynamics simulations of membrane proteins. *Methods* 41:475–488.

[12]2010. AmberTools 1.4. http://ambermd.org.

[13]Ségalas, I., Y. Prigent, D. Davoust, B. Bodo, and S. Rebuffat, 1999. Characterization of a type of β-bend ribbon spiral generated by the repeating (Xaa-Yaa-Aib-Pro) motif: The solution structure of harzianin HC IX, a 14-residue peptaibol forming voltage-dependent ion channels. *Biopolymers* 50:71–85.

[14]Bürck, J., S. Roth, D. Windisch, P. Wadhwani, D. Moss, and A. S. Ulrich, 2015. UV-CD12: synchrotron radiation circular dichroism beamline at ANKA. *J. Synchrotron Rad.* 22:844–852.

[15]Laio, A., and M. Parrinello, 2002. Escaping free energy minima. *Proc. Natl. Acad. Sci. USA* 99:12562–12566.

[16]Barducci, A., G. Bussi, and M. Parrinello, 2008. Well-Tempered Metadynamics: A Smoothly Converging and Tunable Free-Energy Method. *Phys. Rev. Lett.* 100:020603.

[17]Jämbeck, J. P. M., and A. P. Lyubartsev, 2013. Exploring the Free Energy Landscape of Solutes Embedded in Lipid Bilayers. *J. Phys. Chem. Lett.* 4:1781–1787.

[18]Bochicchio, D., E. Panizon, R. Ferrando, L. Monticelli, and G. Rossi, 2015. Calculating the free energy of transfer of small solutes into a model lipid membrane: Comparison between metadynamics and umbrella sampling. *J. Chem. Phys.* 143:144108.

[19]Filipe, H. A. L., M. João Moreno, T. Róg, I. Vattulainen, and L. M. S. Loura, 2014. How To Tackle the Issues in Free Energy Simulations of Long Amphiphiles Interacting with Lipid Membranes: Convergence and Local Membrane Deformations. *J. Phys. Chem. B* 118:3572–3581.